NON-DESTRUCTIVE TESTING OF MAGNETICALLY IMPELLED ARC BUTT WELDING OF MILD STEEL TUBES

M. Chaturvedi[1], S. Arungalai Vendan[1]*, Sharanabasavaraj[1], V. Kachinsky[2], K. A. Ramesh Kumar[3]

[1]Department of Electronics & Communication Engineering, School of Engineering, Dayananda Sagar University, Bengaluru, India
[2]E.O. Paton Electric Welding Institute, Kyiv, Ukraine
[3] Department of Energy Studies, Periyar University, Salem, India
*Corresponding author's e-mail address: arungalaisv@yahoo.co.in, arungalai-ece@dsu.edu.in

ABSTRACT

This paper presents the results of Non-Destructive Testing on Magnetically Impelled Arc Butt (MIAB) welded mild steel tubes of 27mm OD and 1.5mm thickness. As part of this work, the tests covered were radiography, liquid penetrant, and magnetic particle testing. The testing results indicate that porosity, penetration levels and the defects found are within acceptable limits as per standard. For this experimental work, the selection of parameters was based on trial and error adopted in preliminary trials. The irregularities found in the non-destructive testing samples have enabled the fine-tuning of process parameters. The optimum values of hydraulic pressure, weld time and weld current are assessed to be 30-35bar, 5.5s and 150 A, respectively 270 A for this dimension of tubes. This work focuses on the experimental observations of MIAB welding and Non-destructive testing results for MS tubes of the selected dimension, which have not been reported in the existing literature. The achieved input forms the database for the parametric study of this process. The optimum parametric ranges obtained from the results can be extrapolated to be used for joining tubes of different dimensions and can also form the inputs for reaching parameter and response dependency equations.

KEYWORDS: MIAB welding, NDT, MPT, LPT, radiography, MS1018, material joining.

1. INTRODUCTION

1.1. Magnetically Impelled Arc Butt (MIAB) Welding Process

Since the 1980s, Magnetically Impelled Arc Butt (MIAB) welding has been employed in automobile industry for the hollow tubular components such as pneumatic springs, brake rods, shock absorbers and even for safety critical applications like boiler heat exchangers, economiser coils, etc.

MIAB welding involves striking an arc between two coaxially placed tubes. The interaction between the axial component of an arc current and the radial component of an external magnetic field creates Lorentz force. This force acts on the arc and impels it around the joint line with an approximate linear speed of 200m/s that uniformly heats the tube surfaces up to their solidus temperature. The softened faying surfaces are then forced into penetration by forging to form a weld. The schematic figure 1 illustrates the arc impelling mechanism in the MIAB welding process.

The current and the magnetic field interaction is essential for the arc rotation that eventually heats up the faying surfaces. When a current-carrying conductor is placed in a magnetic field, it experiences a force called Lorentz force, equation 1.

$$F = B \cdot I \cdot L_a \quad [N] \tag{1}$$

where B is the magnetic flux density; I - welding current; L_a - length of arc.

In this welding process, the arc is the current-carrying conductor and is acted upon by the Lorentz force which concentrates it in the magnetic field region between the tube surfaces. The Lorentz force and the velocity of the arc are related by equation 2 [1].

$$v_{arc} = \frac{F}{k}\left(1 - e^{-\frac{kt}{m}}\right) \tag{2}$$

where F is the Lorentz force [N]; k - constant of air resistance; m - mass of the arc, [Kg]; t - time [s].
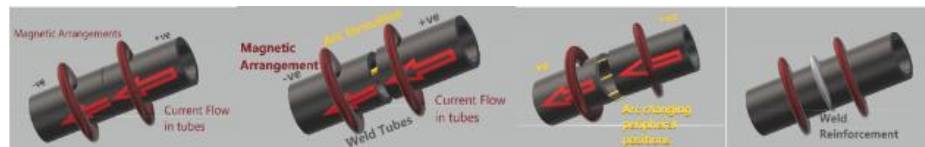
Fig. 1. Arc impelling mechanism in MIAB welding

The force acting on the arc steadily builds its velocity in the peripheral region. The rotating arc then uniformly heats up the tube surface. The temperature rise with the localised heating causes material softening at the tube surface. Then upset force is provided for fusing the softened butt surfaces. This causes surface impurities to melt and get expelled out of the joint surface. These molten impurities get deposited on the surface in the form of a bead.

Thus, the process involves three sequences, viz. arc formation and sustenance, heating and forging. Each of these stages requires different amperage and time duration (Table 1). Current and time values depend on the energy required to bring the material to its solidus temperature and to cause the tubes to coalesce. These ranges, based on experiments by prior researchers, apply to mild steel grade tubes of 20-30 mm outer diameter and 3-6 mm thickness. The time required for this weld is significantly smaller than that required for other solid-state welding processes.

Table 1. Current and time range for MS1018 tubes of 27 mm OD and 1.5 mm thickness in various phases of MIAB welding process

Stage	Current [A]	Time [s]
I: Arc-Formation, Rotation, Heating	140-180	5-5.5
II: Upset Stage	250-270	0.3-0.4

The weld samples are subjected to testing procedures to check their compliance with the ASME/AWS standards. Various Non-Destructive Testing (NDT) techniques are employed to determine the weld quality.

Section 1 of this paper covers the process description, testing techniques and the state of the art. Section 2 describes the experimental setup, parameter selection and the testing procedure for the weld samples. Results and discussions are included in section 3, followed by Conclusions in Section 4.

Investigations on MIAB welding started early in the 1950s in Europe and several research developments further revealed the merits of this process and promoted it as industry-friendly welding technique [3]. Research advancements have been contributing to process development and industrial acceptability from application perspectives.

Peng M. et al [4] reported the efficacy of MIAB welding for dissimilar materials for deployment in automobile components like stabiliser bars. Tubes of 6mm thickness of Ductile Cast Iron (DCI) with

E355+N alloy steel were welded together. Poor weldability of DCI resulted in weld distortions and the peeling phenomenon on employing conventional welding methods. But the MIAB welding technique resulted in efficient weld, with desirable properties of DCI with alloy steel, without the need for any filler material or preheating.

Arc velocity varies in different phases of the MIAB welding process. The heating stage experiences unstable arc velocity [5] and may lead to the quenching of the arc by forming a short circuit between the tube faces. These complications are prominent with larger thickness tubes and thus describe the limitations of this process for application to tubes of thickness larger than 8mm [3] which have restricted its wide adaptability in the manufacturing industry.

Papanikolaou et al [6] reported results of ultrasonic testing of welded steel samples. They suggested improved welding techniques for welding repairs in several critical weld applications. This was based on discontinuities observed in the ultrasonic testing of weld samples. Ultrasonic tests were inferred to be an effective testing method in order to identify discontinuities in the weld sample, compared to Visual Testing, penetrant or magnetic particle testing.

Kustron et al [7] demonstrated the use of scanning acoustic microscopy, fig. 2, to implement subsurface ultrasonic waves testing of the weld samples. Subsurface ultrasonic waves are an efficient way of validating thin-walled tubular weld samples, even without burring the sample.
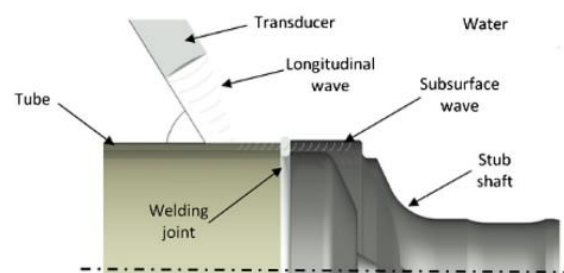

Fig. 2. Subsurface testing methodology [7]

Sedighi et al [8] performed metallurgical studies and used Finite Element Simulation (FES) for the analysis of residual stresses generated in MIAB welded specimens. They observed stress to be proportional to the weld time and inversely proportional to the upset pressure. Welding pressure helps reducing residual stress in the axial direction with no impact on the circumferential stresses. Metallography and the

simulation results showing the microstructural phase content are in agreement with each other as shown in figure 3.
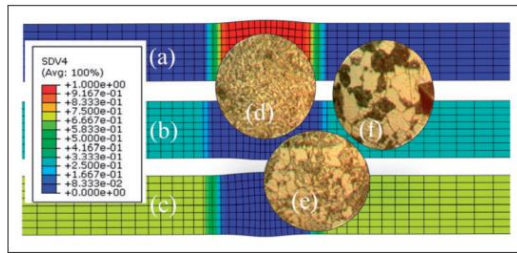

Fig. 3. Distribution of phase content and microstructure of welded joints after cooling: a) bainite; b) pearlite; c) ferrite; d) microstructure of the weld line; e) microstructure of transition zone – HAZ; f) base material microstructure [8]

Sivashankari et al [9] observed the formation of a distinct white zone at the weld as part of the macro examination in samples that are welded with lower upset current. This band zone indicates chemical inhomogeneity caused by incomplete homogenisation and incomplete expulsion of decarburised region at the weld. Tensile tests of such samples show low strength and ductility. Also, the SEM analysis of these samples indicated retention of oxide impurities at the interface.

Arungalai Vendan S. et al [10] studied the use of the MIAB welding process for joining pressure parts like economiser coils of pressure vessels. They suggested that due to the interaction with gas molecules during the upset stage, thin layers of oxides or non-protruding inclusions may be formed that cannot be detected by radiography tests. In the SEM fractography of weld samples, a form of inclusion was observed, which was not revealed in the microscopic images. Also, the tensile test and root-bend test provided varying observations for the fracture to be brittle or ductile. With these studies, they highlighted the significance of individual testing methods in assessing the weld quality.

Iordachescu et al [11] utilised infrared thermography with AGEMA thermo-vision 900 for capturing the rate of change of the thermal gradient during the MIAB welding process. They suggested the use of tube deformation factor ($\delta > 0.5$) for measuring the upset phase deformation as the weld quality indicator. The used an HRDC camera to capture the arc's velocity in this process. The metallographic analysis helped to examine the influence of the tube gap and magnetic induction on the arc rotation and heating duration in the joining process.

Although research work has been reported on experimental, FES, statistical, optimisation and characterisation studies on MIAB welding of tubes, there are still technical ambiguities with respect to defect analysis. Details on destructive analysis are adequately reported. However, reports on NDT methods and defect analysis are exiguous. NDT techniques are utilised for locating faults and imperfections on the surface and subsurface of materials. This further ensures the welding joint conforms to standards and specifications. The MIAB welding still requires detailed process parametric studies in order to establish governing equations and assessment standards for an efficient weld [12]. In an attempt towards this requirement, current experimental work is undertaken. This paper includes an overall description of the welding process and of the non-destructive testing techniques that have been utilised for MIAB welding samples. The experiments have been conducted based on the experimental design and sequential narrowing down of the parametric range, based on the weld sample characteristics. NDT results, based on visual examination, liquid penetrant examination, magnetic particle testing and radiography, demonstrate the process capability in forming efficient welds in thin section ferrous tubes with the established parametric range.

1.2. Testing Procedures

Defects in the weld samples may arise due to improper weld procedures. Identifying the defects provides a way to control the manufacturing process. Non-destructive testing is used in industry to evaluate the quality of a weld without causing damage to the sample. Non-destructive testing includes means of testing a material, detecting the flaws, defects, or irregularities, using an integrated sensor control mechanism for indicating or recording the response and its interpretation. Non-destructive testing methods are effective for weld quality evaluation and early defect detection.

These tests help identify any offsets or mismatch, root undercut, cracks, porosity, holes, incomplete penetration or inclusions in the weld and other such irregularities. Selection of the NDT depends on the product applications, possible defect location or flow type. Detection and evaluation helps in minimising the overall manufacturing cost by pre-empting any fault in the manufacturing of the parts.

1.2.1. Radiography

Radiation in the form of X-rays, gamma rays or neutron beams is passed through the sample and is differentially absorbed depending on the thickness, type of material and the presence of surface defects. Radiated beam experiences higher attenuation for higher atomic number materials. Shadow pattern is subsequently created on a photographic film [14].

This technique (Fig. 4) probes the internal regions of the material and is very sensitive to density changes. Defects must be at least 2% of the total section thickness to be detected. A standard test piece called the penetrameter that has known dimensions is often included in a radiographic exposure for comparative study.
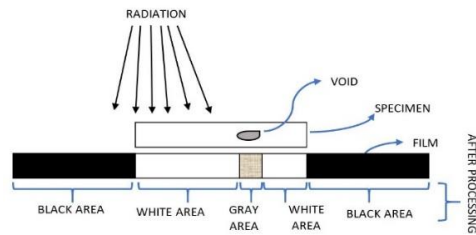
Fig. 4. Radiography Technique

The double wall exposure double view (DWEDV) technique is used on tubes or pipes where the diameter is less than 80 mm. In the DWEDV technique, the radiation passes through both the walls of the object and multiple exposures are needed to accomplish the complete coverage. An image of both the upper and lower parts of the weld is projected by offsetting the source from the weld center line and a long source is used to film the distance. The source of radiation may be positioned directly over the area of interest, thus superimposing the top portion with the region directly under it. As an alternative, the source may be offset by an angle of approximately 15^0 in order to observe both the top and bottom walls. The quality of the radiograph is examined using three features: contrast, density and sharpness of the image.

1.2.2. Liquid penetrant inspection

Liquid penetrant test checks for flaws in the material that is open to the surface. These irregularities are detected by forcing a very thin liquid into the surface and then drawing it out using a developer.

This is a swift and economical inspection method for detecting even small surface discontinuities. This process is portable and can be used to detect the relative size, depth, and shape of the flaw. It can be used to inspect metallic, non-metallic, and non-conductive or even magnetic materials [15].

Procedure of LPT (Fig.5) as per ASME Section V Article 6, T676.1 is as follows [2]:
1. Surface preparation was performed to free the weld sample from dirt, rust, scale, paint, oil, and grease, and to make it smooth enough to wipe off the penetrant without leaving residue. This was followed by grinding and wire brushing or merely wiping the part with a rag moistened with cleaner/ remover, as it may be required.
2. Penetrant was applied by spraying it from the aerosol can or by applying it with a brush.
3. Penetrant is left on the surface to permeate into cracks and voids. This duration is termed as dwell time and is typically of the order of 5 to 30 minutes, while making sure that the penetrant does not dry.
4. Excess penetrant is removed with clean, dry, lint-free rags until it is thoroughly cleaned. Solvents like water or water-soluble emulsifiers were used for removing excess penetrant. The exposed part or material is vigorously rubbed until the penetrant is not visible on the dry rags.
5. A thin, light developer coating is sprayed on the part that is being examined. A dwell time was observed that allows the dye to exit the flaws and create an indication (flaw) in the developer. The dwell time for the developer is typically 10 to 60 minutes.
6. Inspection was done with minimum light requirement of 1000 Lux – the part is examined within the time frame designated in the standards. Length of an indication can grow over time as the penetrant bleeds out, causing an acceptable indication to be a rejectable defect.
7. Flaws may be indicated in various ways. Lines indicate cracks, seams, or incomplete fusion. Dots in a line or in a curve may indicate a tight crack or porosity.
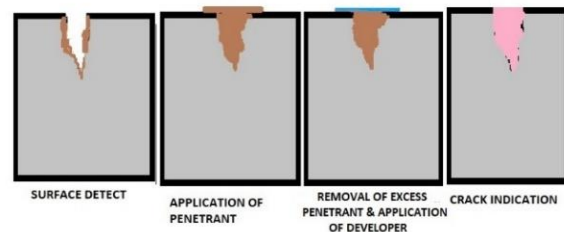

Fig. 5. Liquid Penetrant Test

1.2.3. Magnetic Particle Testing

When magnetic field lines are made to pass through defect free ferromagnetic materials, no distortion is observed in the transfer lines. In the presence of a crack or other discontinuity, magnetic flux leaks from the material are distorted at those spots of surface or subsurface discontinuities. Magnetic flux leakage will be observed only in case of cracks which are perpendicular to its flow. Magnetic particles in the form of dry powder or suspension in liquid, will be strongly attracted to those regions where the magnetic flux breaks the surface. This collection of magnetic powder or suspension makes the size and share of the discontinuity easily visible.

This testing method is commonly employed for defect detection in the steel tubes and pipes in pressure parts. This technique is sensitive to cracks that block the path of magnetic field. Magnetic field is induced in different orientations, Fig. 6. AC supply is used to detect surface flaws, while DC supply is preferred for subsurface defects like non-metallic inclusions. For surface open defects, AC is preferred whereas for deeper penetration defect checking, straight DC or rectified half wave and full wave supply is used. AC induced magnetic field has a scale effect that produces a concentrated field on the surface [16]. Magneto-optical imaging under a vertical combined magnetic field [17] can accurately detect weld defects of any shape and orientation.
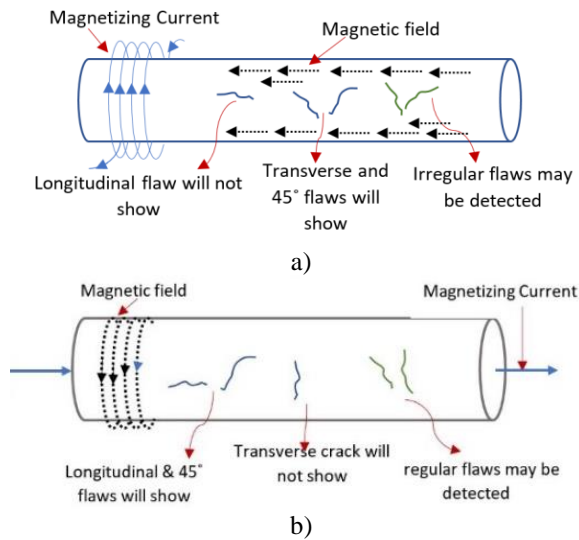
Fig. 6. Magnetisation methods: a) longitudinal magnetisation; b) circular magnetisation

As per inspection standards, ASME Section-V, Article-7 (magnetic particle examination) and SE709 (standard practice for magnetic particle examination) and ASME Section-VIII, Division 1, the procedure followed for MPT is as follows:

- Surface to be examined and all adjacent areas within one inch on both sides of the weld edge are dried and cleaned from impurities and extraneous materials like dirt, grease, lint, scale, welding flux, spatter that could interfere with the examination.
- Examination medium - the ferromagnetic particles to be used as an inspection media can be wet or dry and may be either fluorescent or visible. Fluorescent media is more sensitive to defects or cracks. Powder dispenser bulb for dry magnetic powder and aerosols for wet inks are used. Magnetic medium in wet systems have pigments that fluoresce at 365 nm, which requires 1000 lux of black light applied for proper inspection. Iron oxide is a commonly used material in both wet and dry systems.
- Magnetization of the test plate and inspection - Electromagnetic yoke energised with alternating current or direct current is placed on the welded surface along and later across the weld surface to detect cracks and other discontinuities.
- The defects may be oriented perpendicular or nearly perpendicular to the lines of magnetic flux. Magnetic particles are applied on a part of the specimen while the current in the electromagnetic yoke is flowing.
- Magnetizing field strength was determined by the lifting power of the yokes (4.5 kg and 18 kg weights for alternating and direct current respectively).
- Formation of the clearly defined lines due to

accumulation of the magnetic particles over the surface of the indicator reveals the desired adequacy of the technique.
- Examination was conducted in succession with sufficient overlap to cover 100% of the area at required sensitivity.
- Discontinuities on the surface are indicated by retention of the examination medium.
- The maximum sensitivity is for defects in transverse orientation to the magnetic field lines.
- Size, number and location of all linear and round indications (with size above 1.6 mm) is recorded.

MPT test results are reported on the basis of observation of linear or round recordable indications. Linear indication refers to that indication whose length is more than three times its width. Round indications point out those irregularities in which length is equal or less than three times their width.

2. EXPERIMENTAL TRIALS AND TESTS

2.1. Experimental Setup

Experiments were carried out on the MIAB welding setup available at Dayananda Sagar University, Bangalore. The setup, from figure 7a, includes a power supply module, control panel for current and time settings, hydraulics and the welding unit. The weld sample holders, (Fig. 7b), in this machine accommodate tubes of 27 mm OD. Pressure required in the upsetting stage is generated by a hydraulic system supplemented by a nitrogen accumulator that drives the axial movement of one weld head. The hydraulic system, figure 7c, includes hydro motor, pressure sensors, cylinders, pipeline and sleeves of high pressure. This mechanism works by controlling the flow of hydraulic oil HP grade 46 at the defined pressure of 40 bar, that is specific to the material properties. This system causes retraction of the tubes in the initial stage for arc creation, which is enabled by the controlled flow of working fluid in the hydro-cylinders [13]. Hydraulic arrangement is pre-programmed to forge the tubes together at a pressure of 30-40 bar. In the preliminary experimental trials, it was observed that at any pressure beyond and below this range, the weld sequence does not get implemented.

In this study, weld trials were performed on MS1018 mild steel tubes (27mmOD, 1.5mm thickness) whose chemical composition is shown in Table 2.

Table 2. Chemical composition of the MS1018 weld samples

Element	C	Si	Mn	P	S
Wt [%]	0.14-0.20	0.15	0.6-0.9	0.04 (max)	0.05 (max)

Fig. 7. Experimental Setup: a) machine setup; b) welding heads; c) hydraulic system

2.2. Parameter Value Selection

The values of current, time and pressure depend on the weld machine specifications, material properties and its geometry. The selection of process parameters for the welding of MS1018 tubes is based on preliminary experimental work on the new fabricated MIAB welding machine and on the trial-and-error method. The trials were made with different ranges based on reported results for other dimensions of tubes [3], [9].

The first set of trials involved experiments for reaching the required hydraulic pressure and stage I current. Operational range of the second stage current and time duration settings for both the stages were then correspondingly adopted. Further optimisation was then essential for achieving higher weld efficiency and also for optimal energy consumption. The following experiments helped in reaching an optimum range for the selected material and dimensions.

2.3. Non-Destructive Testing Techniques

Following the experimental trials, the non-destructive tests (NDT) were carried out on the samples. NDT tests were carried out at Matrix, Engineering Inspection Services, Hosur, an NABL certified lab for material testing. For the MIAB welded tubes with diameter of less than 38mm diameter, ASTM E1032-19 standard was followed. ISO 23277, ASTM E 165 and ASME BPV Section V Art.6 were adopted for implementing the LPT for weld samples. ASTM E3024/E3024M -19e1 was followed for MPT on the weld samples.

2.3.1. Radiography Testing

Tests were carried out on MIAB welds with and without the reinforcements. Grinding is done to remove the reinforcement and the weld area is cleaned before subjecting to radiography test. Radiography testing was carried to identify and analyse the defects in the MIAB welded joint with the specifications from table 7.

2.3.2. Liquid Penetrant Testing

Liquid Penetrant test was carried with the following

specifications from table 9. First stage of the test involves applying penetrant to the sample (Fig. 8).

Fig. 8. Specimen during LPT on penetrant application

2.3.3. Magnetic Property Testing

These set of tests were carried out using the specifications from table 11.

3. RESULTS AND DISCUSSIONS

3.1. Experimental Results

Table 3 presents the parameter values and weld results obtained for the hydraulic pressure between 30 to 35 bar. As observed from table 3, for the pressure range of 30-35 bar, the weld sequence got completed without the arc creation. This indicates the pressure of 30-35 bar is insufficient for causing the weld of 27mm OD MS1018 tubes with this process. A second set of trials were performed with increased pressure, while maintaining Stage I current and stage II current and time durations for both stages same as the experimental set 1. The results of this test are reported in table 4.

Table 3. Experimentation Phase I.
Input parameters and observations

Tube Outer Diameter – 27 mm, Hydraulic Pressure – 30 ÷ 35Bar, Nitrogen Accumulator Pressure – 30 Bar.					
Sample	I_1 **[A]**	I_2 **[A]**	T_1 **[s]**	T_2 **[s]**	**Remarks**
1	140	270	5	0.3	No arcing due to low hydraulic pressure
2	145	270	5	0.3	
3	150	270	5	0.3	

4	155	270	5	0.3
5	160	270	5	0.3
6	165	270	5	0.3
7	170	270	5	0.3
8	175	270	5	0.3
9	180	270	5	0.3

Table 4. Observation table for varying stage I. Current for increased hydraulic pressure.

Tube Outer Diameter – 27mm,
Hydraulic Pressure – 35÷40 Bar,
Nitrogen Accumulator Pressure – 30 Bar.

Sample	I_1 [A]	I_2 [A]	T_1 [s]	T_2 [s]	Remarks
1	140	270	5	0.3	Arc formed between the tubes, but immediately extinguished. Nitrogen accumulator pressure maintained same as hydraulic pressure.*
2	145	270	5	0.3	
3	150	270	5	0.3	
4	155	270	5	0.3	
5	160	270	5	0.3	
6	165	270	5	0.3	
7	170	270	5	0.3	
8	175	270	5	0.3	
9	180	270	5	0.3	

* Result: arc extinguished due to short circuit with the pressure of weld heads bringing the tubes together.

Based on the observations made from Table 4, further trials were attempted with higher pressure difference by reducing nitrogen accumulator pressure and increasing hydraulic pressure. Table 5 lists the results of various parametric combinations with lowered nitrogen accumulator pressure.

Table 5. Trials based on reduced hydrogen accumulator pressure

Tube Outer Diameter – 27 mm,
Hydraulic Pressure – 34 ÷ 40Bar,
Nitrogen Accumulator Pressure – 20 Bar.

Sample	I_1 [A]	I_2 [A]	T_1 [s]	T_2 [s]	Remarks
1	140	270	5	0.3	No arc
2	145	270	5	0.3	No arc
3	150	270	5	0.3	Arcing with incomplete rotation
4	155	270	5	0.3	Arcing with complete rotation, weld achieved
5	160	270	5	0.3	
6	165	270	5	0.3	
7	170	270	5	0.3	Melting of impurities in the weld region and formation of bead due to high current
8	175	270	5	0.3	
9	180	270	5	0.3	

The third set of experimental trials helped reach a suitable working range of pressure and stage I current with other parameters maintained constant at appropriate levels. Samples were further made with the lower subrange of current with the intention to reduce the energy input of the process. These samples were then subjected to mechanical tests to verify the desired weld characteristics.

Table 6 lists the parametric variations and shows the weld formation for each sample. From the above iterations, appropriate operating ranges of pressure, current and time for 27 mm OD and 1.5 mm thickness MS 1018 tubes have been arrived at. The weld interface is observed to have better mechanical properties as compared to the base metal.

Table 6. Weld formation and mechanical testing result with the lower variation in parametric range

Sample	I_1 [A]	I_2 [A]	T_1 [s]	T_2 [s]	Weld Formation
1	155	270	5	0.3	
2	157	270	5	0.3	
3	158	270	5	0.3	
4	159	270	5	0.3	

MIAB welded tubes with the flash (reinforcement) is shown in figure 9. MIAB welded tubes without flash is shown in figure 10. In this sample, the flash/reinforcement is grinded.

Fig. 9. MIAB Weld Sample with reinforcement

Fig. 10. MIAB Weld Sample without the reinforcement

3.2 NDT Results
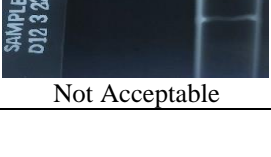
3.2.1. Radiography

Results of the tests are recorded in Table 8. as per ASME Section VIII Div 1. Acceptability of these tests results is based on QW-191.1.2.2 standard in ASME Section IX. Crack and incomplete fusion is considered unacceptable. The length of elongated inclusion depends on the test piece thickness. Any elongated slag inclusion will be unacceptable if the length is more than 1/8 inch when the thickness of the specimen is between 0 and 3/8 inch.
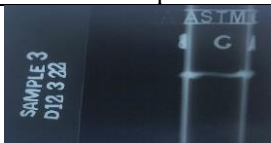
Table 7. Radiography Specifications

Ref. Code	**ASME SEC V Ed 2020**
Acceptance Criteria	**ASME B 31.3; Ed 2020**

Source & Activity	X-Ray, 300KV, 5mA
Source Size	2.5" *2.5"
Sensitivity	<=2%
I.Q.I Type	SET-A (1 A 06)
Screens	0.125mm Pb/0.125mm Pb
Devlp. Time & Temp	3-6 min 18˚-24˚C
Film Type and Size,	AGFA D-5, 4" *6"
FFD	25"
Exposure Time	3.5 minute
Optical Density	2.6
Technique	DWDI

Table 8. Radiography Results

Sample	I_1 [A]	I_2 [A]	T_1 [s]	T_2 [s]	Segment	Observation	Result
1	155	270	5	0.3	A	Pore	Not Acceptable
					B	Pore	Not Acceptable
					C	Pore	Not Acceptable
2	156	270	5	0.3	A	Slag Inclusion	Not Acceptable
					B	Slag Inclusion	Not Acceptable
					C	Slag Inclusion	Not Acceptable

Sample	I_1 [A]	I_2 [A]	T_1 [s]	T_2 [s]	Segment	Observation	Result
3	157	270	5	0.3	A	No Significant Defect	Acceptable
					B	Excess Penetration	Not Acceptable
					C	Slag Inclusion	Not Acceptable
4	158	270	5	0.3	A	Slag Inclusion	Not Acceptable
					B	No Significant Defect	Acceptable
					C	No Significant Defect	Acceptable

Samples with arc current of 157A (segment A) and 158 A (segments B, C) are found to be acceptable as per the standards. These samples did not exhibit formation of pores, slag inclusion in the weld interface or excess penetration of the coalescing surfaces. Sample without the reinforcement shows reduced porosity, indicating high concentration of pores in the reinforcement region and not in actual weld line. Acceptable results from radiography will be obtained for an impurity free butt joint with the reinforcement removed. Pores may be present due to the interaction of the gas molecules in the weld region during the heating and cooling cycles experienced along the weld periphery. These could be eliminated by employing shielding gas. Though the porosity levels result in acceptable radiography results in some of the samples, this test fails to detect thin layers of oxide or flattened inclusion at the weld line. These impurities may result in weak welds due to areas of incomplete adhesion, thus radiography must be supported by additional tests for a comprehensive idea on the quality of MIAB welds.

3.2.2. Liquid Penetrant Test

LPT observations are listed in Table 10. LPT revealed acceptable results with no recordable pore for arc current of 157 and 158A. Indications with dimension greater than 1.6 mm are considered a relevant defect. Sample welded with 155A arc current had a recordable indication, but within acceptable limits, while Sample 2 with 156 A arc current had a recordable indication pore. Further, the results indicated no porosity inferring uniform and appropriate heating of the weldments. Porosity indicates formation of voids, which can be due to non-uniform heating resulted by inappropriate current levels and heating time duration.

3.2.3. Magnetic Particle Testing

Results from the MPT are recorded in Table 12. MPT results indicate acceptable welds for samples 2, 3 and 4 with arc current of 156, 157, 158A respectively. Sample 1 with arc current of 155A, is reported to have a linear indication in the weld. Discontinuity in the weld results in the magnetic flux leakage, which

produces the linear indication in this test. This result indicates presence of a deep penetrated crack in the weld. The presence of the crack indicates that during the weld process the cooling of the material was faster than the time that is required for uniform solidification. This further points to non-uniform heating due to inappropriate propelling of the arc. This observation is explained by the rise in the process temperature during the weld, which causes de-intensification of the

magnetic field lines. Also, this reduces the Lorentz force acting on the arc. Indication was observed with lower value of arc current, which reinstates significance of appropriate arc current in the presence of a fixed magnetic field and the arc length. With larger current values, the interaction of magnetic field and the arc current creates the required force to ensure required arc speed and the uniform heating created along the circumferential surface.

Table 9. LPT specifications

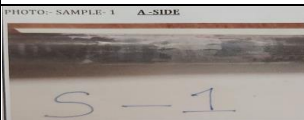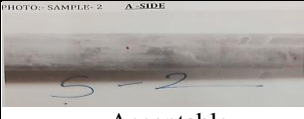| Ref. Code	Acceptance Criteria	Penetrant	Cleaner	Dwell Time	Development Time	Illumination
ASTM E165 / E165M:2021	ASME SEC VIII DIV.1, APPX 8: 2021	Ferro Chem. FC711/2	Ferro Chem. FC811/2	15 min.	10 min.	1473 Lux

Table 10. LPT observations
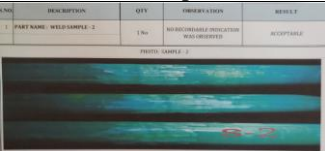
Sample	I_1 [A]	I_2 [A]	T_1 [s]	T_2 [s]	Observation	Result
1	155	270	5	0.3	Linear recordable indication	Acceptable
2	156	270	5	0.3	Weld had recordable indication of pore	Not acceptable
3	157	270	5	0.3	No recordable pore	Acceptable
4	158	270	5	0.3	No recordable pore	Acceptable

Table 11. MPT Specifications

Ref. Code	ASTM E709/E709M
Acceptance Criteria	ASME SEC VIII, Div. I App-6
Method	Fluorescent-Wet
Magnetisation Method	Longitudinal
Magnetisation Current	DC
Field Strength	18.0 Kg
Pole Spacing	4"-6"
Light Intensity	UV Light 1247µW/cm^3
Surface Temperature	Ambient

Table 12. MPT Results

Sample	I_1 [A]	I_2 [A]	T_1 [s]	T_2 [s]	Observation	Result
1	155	270	5	0.3	Linear Indication was observed	Not Acceptable
2	156	270	5	0.3	No Linear Indication was observed	Acceptable
3	157	270	5	0.3	No Linear Indication was observed	Acceptable
4	158	270	5	0.3	No Linear Indication was observed	Acceptable

4. CONCLUSIONS

This work reports the experimental observations made in the MIAB welding of MS1018 tubes of 27 mm OD and 1.5 mm thickness. Radiography, magnetic particle testing and liquid penetrant testing have also been done as part of this work.

The experimental findings and the non-destructive testing results for welded MS tubes of the selected dimension have not been reported in the existing literature. These findings will be significant for arriving at parametric dependencies and for framing standards and codes for this relatively new welding process. The experimental trials that were carried out have helped in achieving the operating ranges of process parameters. The initial and continuing performance of the MIAB weld machine and continuing quality of the materials were ensured with the results from the non-destructive tests. Irregularities observed as part of the tests help in reaching the parametric range for crack free weld formation, for the considered geometry of MS1018 material. Operating range for the 2 stage currents and the time are: Arc current of 156-158A, upset current of 270A, and time durations of 5 and 0.3 s. With the current and time settings at their appropriate levels, the variations in the MIAB joint formed can be attributed to the following factors:

- Irregularities in the weldment
- Non optimum force acting on the arc
- Variations in upset pressure
- Rate of application of pressure
- Magnetic properties of the AlNiCo or ferrous magnets
- Tube gap length
- Thermal conductivity of the material

Further research in this field must provide optimal parametric range for different materials of various dimensions. They must also focus on reliability and reproducibility of the weld characteristics on every iteration. The observations made as part of this work and further research will help establish the MIAB weld process as a preferred industrial joining method for ferrous tubes over other conventional solid-state processes.

ACKNOWLEDGEMENTS

REFERENCES

[1] **Taneko A., Arakida F., Takagi K.,** *Analysis of arc rotation velocity in magnetically impelled arc butt welding*, Welding International, 1987, vol 1. iss. 3, pp. 247-253.

[2] ******* American Society of Manufacturing. Metals handbook, *Nondestructive evaluation and quality control*, vol. 17, 9th ed. ,New York, USA.

[3] **Vendan S. Arungalai, Manoharan S., Buvanashekaran G., Nagamani C.**, *Development of a MIAB welding module and experimental analysis of rotational behavior of arc—simulation of electromagnetic force distribution during MIAB welding of steel pipes using finite element analysis*, The International Journal of Advanced Manufacturing Technology, vol. 43, iss. 11-12, 2009, pp. 1144-1156.

[4] **Peng M., Liu H., Xuan Y., Liu X., Xu L., Yu Z.**, *Evaluation of the microstructural and mechanical properties of ductile cast iron and alloy steel dissimilar materials welded by magnetically impelled arc butt*, Journal of Materials Research and Technology, vol. 15, 2021, pp. 4623 - 4635.

[5] **Sivasankari R., Balusamy V., Venkateswaran P. R., Buvanashekaran G., Kumar K. G.**, *Characterization of magnetically impelled arc butt welded T11 tubes for high pressure applications*, Defence Technology, 2015, vol. 11, iss. 3, pp. 244-254.

[6] **Papanikolaou S., Fasnakis D., Maropoulos A., Giagopoulos D., Maropoulos S., Theodoulidis T.**, *Non-destructive testing of welded fatigue specimens*, MATEC Web of Conferences, 2020, vol. 318, p. 01033.

[7] **Kustroń P., Korzeniowski M., Piwowarczyk T., Sokołowski P.**, *Application of Immersion Ultrasonic Testing for Non-Contact Quality Evaluation of Magnetically Impelled Arc Butt Welded Drive Shafts of Motor Vehicles*, Advances in Automobile Engineering, 2017, DOI: 10.4172/2167-7670.1000161.

[8] **Sedighi M., MosayebNezhad, J.**, *The influence of process parameters on the distribution of residual stresses in magnetically impelled arc welded joints*, Proceedings of the Institution of Mechanical Engineers, Part C: Journal of Mechanical Engineering Science, vol. 233, iss. 11, 2019, pp. 3936-3949.

[9] **Sivasankari R., Balusamy V., Venkateswaran P. R., Kumar K. G., Buvanashekaran G.**, *Light band zone formation and its influence on properties of magnetically impelled arc butt (MIAB) welded carbon steel tubes*, Transactions of the Indian Institute of Metals, vol. 71, iss. 2, 2018, pp. 351-360.

[10] **Arungalai Vendan S., Mundla S., Buvanashekaran G.**, *Feasibility of magnetically impelled arc butt (MIAB) welding of high-thickness tubes for pressure parts*, Materials and Manufacturing Processes, vol. 27, iss. 5, 2012, pp. 573-579. DOI: 10.1080/10426914.2011.585488.

[11] **Iordachescu D., Georgescu B., Iordachescu M., Lopez R., Miranda R. M., García-Beltrán A.**, *Characteristics of MIAB welding process and joints*, Welding in the World, vol. 55, iss. 1, 2011, pp. 25-31.

[12] **Singh P. K., Singh R. P.**, *In-Pressure Magnetically Induced Arc Butt Welding of Alloy Steel Tubes*, in: Manik G., Kalia S., Verma O. P., Sharma, T. K., Recent Advances in Mechanical Engineering. Lecture Notes in Mechanical Engineering, Springer, Singapore, 2023.

[13] **Arungalai Vendan S., Thangadurai V., Vasudevan A., Senthil Kumar A.**, *Investigations on temperature distribution during revolutionary and zigzag movement of arc in magnetically impelled arc butt welding of tubes*, International Journal of Applied Electromagnetics and Mechanics, vol. 46, iss. 1, 2014, pp.155-163.

[14] **Charles J. Hellier**, *Handbook of Non Destructive Evaluation*, McGraw-Hill Publication, New York, 2003.

[15] **Endramawan T., Sifa A.**, *Non Destructive Test Dye Penetrant and Ultrasonic on Welding SMAW Butt Joint with Acceptance Criteria ASME Standard*, IOP Conference Series: Materials Science and Engineering, vol. 306, no. 1, 2018, p. 012122.

[16] **Zolfaghari A., Zolfaghari A., Kolahan F.**, *Reliability and sensitivity of magnetic particle nondestructive testing in detecting the surface cracks of welded components*, Nondestructive Testing and Evaluation, vol. 33, iss. 3, 2018, pp. 290-300.

[17] **Ma N., Gao X., Tian M., Wang C., Zhang Y., Gao P. P.**, *Magneto-Optical Imaging of Arbitrarily Distributed Defects in Welds under Combined Magnetic Field*, Metals, *12*(6), 2022, p. 105.